



Characterization of soil trace metal pollution, source identification, and health risk assessment in the middle reaches of the Guihe River Basin

Zongjun Gao · Menghan Tan · Jiutan Liu ·
Yuqi Zhang · Yiru Niu · Bing Jiang

Received: 2 September 2023 / Accepted: 29 December 2023 / Published online: 9 January 2024
© The Author(s), under exclusive licence to Springer Nature Switzerland AG 2024

Abstract The natural environment, as well as human production and survival, is intrinsically dependent on soil. This study comprehensively assessed the pollution status, health risks, and sources of trace metals in the middle reaches of the River Gui Basin (MRGB) utilizing the geoaccumulation index, potential ecological risk index (PERI), and human health risk evaluation method. The findings of this study provide the following key insights: (1) only Cu and Pb levels in the MRGB soils did not exceed the background values established for soils in Weifang City (WFC). (2) The geoaccumulation status in most areas of the MRGB ranged from non-polluted to mildly polluted, with the overall ecological risk classification ranging from mild to moderate. (3) The cumulative non-carcinogenic risk for humans in the MRGB remained within acceptable limits, whereas the carcinogenic risk indices fell within tolerable levels. Oral ingestion emerged as the primary exposure pathway for both non-carcinogenic and carcinogenic health

risks. (4) Cu, Zn, Ni, and Cr concentrations in MRGB soils primarily stemmed from natural sources associated with parent rocks, with Zn exhibiting additional influence from anthropogenic factors. In contrast, Pb, Cd, Hg, and As concentrations were predominantly driven by anthropogenic sources. Although the soils in the MRGB typically exhibited mild-to-moderate contamination levels, the contamination levels of Hg and Cd were notably more severe. As and Cr were significant health hazards. Most soil contamination sources are attributed to anthropogenic factors, warranting heightened attention from the relevant authorities.

Keywords Soil trace metal · Pollution characterization · Health risk assessment · Source identification · The middle reaches of the Gui River Basin

Supplementary Information The online version contains supplementary material available at <https://doi.org/10.1007/s10661-023-12280-9>.

Z. Gao · M. Tan · J. Liu (✉) · Y. Zhang · Y. Niu
College of Earth Science and Engineering, Shandong
University of Science and Technology, Qingdao 266590,
Shandong, China
e-mail: ljtsdust@sdust.edu.cn

B. Jiang
No.4 Exploration Institute of Geology and Mineral
Resources, Weifang 261021, China

Introduction

Soil is a pivotal component of human life and serves as a vital nutrient source for plants, a stabilizing agent for environmental changes, and a resource for water preservation. However, it is also a site where numerous pollutants accumulate (Naveedullah et al., 2013). Many environmental contaminants accumulate in the soil and pose significant risks to the soil environment. Among these contaminants, trace metal pollution is particularly detrimental to the soil health (Chen et al., 2005; Govil et al., 2008).

Numerous domestic and international studies have yielded positive results in the investigation of soil trace metal pollution. In Moscow, where potential contamination sources exist, certain forested regions and areas near human-made structures maintain acceptable levels of trace metal contamination in the soils. Nevertheless, human activities significantly influence soil pollution (Guseva and Petrov, 2023). Taghipour et al. (2013) conducted a quantitative analysis of 46 soil samples from the outskirts of a northwestern Iranian city, revealing the impact of the city on adjacent agricultural zones through controlled experiments. Muhammad (2022) employed the ecological risk index (ERI), pollution load index (PLI), and Medalus model to characterize land degradation in Southeastern Serbia, offering a robust methodological foundation for land management. Delavar and Safari (2016) investigated the spatial distribution of Pb, Cu, and Zn near a zinc plant in Zanjan, Iran, identifying intense trace metal contamination near the factory and spreading outward in all directions from its center. A study of soil trace metal contamination in a Malaysian industrial city indicated a gradual decrease from the industrial and residential sectors to rural areas (Hossain et al., 2015). Jadoon et al. (2020), and Din et al. (2022) assessed the distribution and potential risks of trace metals in Pakistani soils by utilizing the load contamination index and human health risk assessment methodology, highlighting a higher susceptibility to carcinogenic risks in children than in adults. Ullah and Muhammad (2020) explored trace metal contamination and phytoremediation potential in soils and plants in Baluchistan, Pakistan, attributing geological sources as the primary cause. Khan et al. (2020) investigated trace metal risks in particulate matter from residential and industrial sites in Islamabad, Pakistan, identifying oral ingestion as the primary exposure route, with children at higher risk than adults. In the Hassimessaoud area of Algeria, industrial sectors exhibited higher trace metal concentrations than rural areas (Mohammed et al., 2014). Lead primarily originates from human activities, such as mining, while nickel and copper are primarily derived from the soil matrix, mining, and agricultural practices (Yang et al., 2022; Sun et al., 2010). Lee et al. (2020) quantified anthropogenic impacts on trace metal contamination in Korean soils using multiple contamination indices and cluster analysis based on a nationwide survey.

The significant presence of soil trace metal pollution in the MRGB is a matter of grave concern owing to its extensive industrial, agricultural, and human habitation significance. As the local economy has grown, there has been a notable increase in pressure due to environmental soil contamination, particularly in recent years. However, previous studies in the MRGB have predominantly focused on crops and agro-economics, neglecting comprehensive investigations into soil pollution characterization, health implications, and contamination sources. Therefore, this study rigorously examined the soil trace metals in the MRGB using conventional geochemical evaluation techniques. We investigated the geographical distribution of trace metals, assessed health-related concerns, and identified the pollution sources of soil trace metals in the region. We aimed to determine the current levels of soil trace metal pollution in the MRGB, its sources, and the potential risks to human health. This study can significantly affect efforts related to soil trace metal pollution prevention and control, ecological environmental protection, and population health within the MRGB.

Materials and methods

Study area

The MRGB, situated at the center of the Shandong Peninsula, exhibits varying topographies with high and low areas in the north, west, and east. It has a mild temperate, semi-humid climate, characterized by distinct seasons. The mean annual temperature is 12.3°C, while annual precipitation and evaporation average 792.5 mm and 1912 mm, respectively. Geologically, the stratigraphy of the Changle County aligns with the Luxi stratigraphic division within the North China stratigraphic zone. Various boundaries such as the Neo-Paleocene, Neo-Paleozoic, and Neo-Cenozoic are distributed throughout the region. Predominantly, Changle County features acidic rocks, with concentrated development of intrusive rocks in the southern and southeastern regions, whereas basal and neutral rocks occur in packages or veins. The Changle is located within the North China Plate of the Lusi Rise and Jiao Liao Rise and is characterized by an active tectonic fault system. According to the hydrogeological zoning of Shandong Province, the northern part of Changle County falls within the loose salt hydrogeological zone of the

Northwest Lu Plain, and the southern part belongs to the carbonate-based hydrogeological zone in the middle and low hills to the south of Lu. Soil types in the region predominantly include tidal, coarse bone, brown, and brown soils. Figure 1 shows a visual representation of the location of the MRGB.

Samples collection and processing

A total of 98 soil surface samples were collected in the MRGB using a grid arrangement based on a 1:50,000 land-use status map. The average sampling density was 5 pieces/km², with samples collected at a depth of 0–20 cm. In four equal portions, the root system, straw, stones, insect remains, and other detritus were removed to maintain a weight between 1 and 1.5 kg in a clean, sturdy cotton bag. Subsequently, a mixed-sample field collection approach was employed for sample deployment.

For rectangular-shaped sampling plots, sub-sample points were arranged in an “S” shape, while square-shaped plots utilized an “X” or checkerboard layout. In the case of a rectangular sample plot, the sub-sampling points were arranged in an “S” shape. For approximately square sampling plots, sub-sampling points were arranged in either an “X” shape or a checkerboard shape. The roughly square sampling plots were maintained at the exact same sampling location, depth, and weight. The soil samples were collected from the wild, naturally air-dried, crushed using a wooden stick, and then passed through a 10-mesh nylon sieve, resulting in 500 g sieved samples. Throughout the soil collection, air drying, grinding, transportation, and storage processes, precautions were taken to prevent any contact with metal utensils that could lead to contamination. Soil pH values were determined using a magnetic PXSJ-226 electrode (Shanghai Yidian Scientific Instrument Co., Ltd.), while

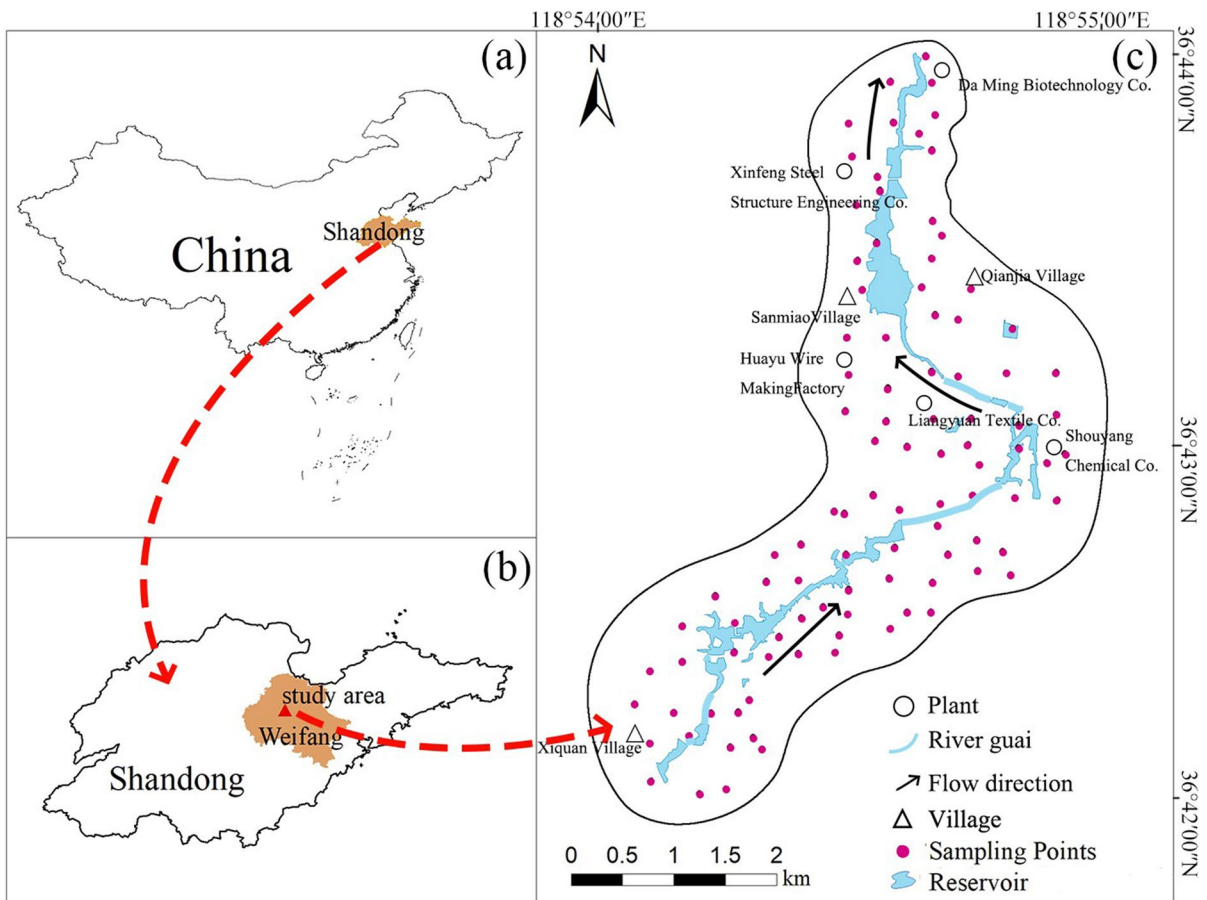


Fig. 1 Geographic overview of the middle reaches of the Gui River Basin

the As and Hg contents were analyzed using an atomic fluorescence spectrometer (AF-630A). The Cu, Pb, Zn, Ni, Cr, Cd, V, Mn, P, and K contents in the soil samples were quantified using an inductively coupled plasma mass spectrometer (Nexlon 2000) (Shanghai PerkinElmer Instrument Co., Ltd.).

To maintain stringent quality control during testing and analysis, a standard substance was included for every 50 soil samples, in line with the quality criteria outlined in the Specification for Geochemical Evaluation of Land Quality (DZ/T0295-2016). This process yielded an accuracy and precision of 100%. In addition, to assess the relative deviation (RD), one duplicate sample was introduced for every 50 samples, resulting in a statistical pass rate exceeding 97%.

Assessment of trace metal pollution

The primary method for assessing soil trace metal contamination involves comparing contamination levels with established reference values. Therefore, selecting appropriate parameters is imperative for accurately evaluating pollution. In this study, both the geoaccumulation index and PERI methods utilized the WFC background values as reference benchmarks. The following values were employed for Cd (0.081 mg·kg⁻¹), Hg (0.015 mg·kg⁻¹), As (8.1 mg·kg⁻¹), Pb (20.3 mg·kg⁻¹), Cr (65 mg·kg⁻¹), Cu (20.1 mg·kg⁻¹), Ni (27.7 mg·kg⁻¹), and Zn (52.8 mg·kg⁻¹) to assess the level of trace metals contamination in the soil and its associated risks.

Geoaccumulative index method and enrichment factor

The geoaccumulation index, also referred to as the Muller index, provides a comprehensive assessment of environmental impacts such as natural geological processes and human activities (Tian et al., 2017). The correction coefficient, denoted as “K,” is commonly used to account for variations in background values resulting from differences between soil and rock properties and is typically set at 1.5 (Lin et al., 2001). The formula is as follows:

$$I_{\text{geo}} = \log_2(C_i/K \times C_{Bi}) \quad (1)$$

where I_{geo} is the ground accumulation index of trace metal i ; C_i is the measured value of trace metal i in soil (mg·kg⁻¹); C_{Bi} is the background value of trace

metal i (mg·kg⁻¹), with the background value of soil in Weifang City as the reference value. The evaluation process is displayed in Fig. S1.

Reimann and Caritat (2005) employed an enrichment factor approach to evaluate soil trace metal enrichment and the presence of anthropogenic sources. This method relies on the ratio between the average trace metal concentration and background soil value. As established by previous studies (Flora et al., 2009), an enrichment factor exceeding 1.5 indicates the presence of anthropogenic sources for soil trace metals.

PERI methodology

The PERI, developed by Swedish scientist Hakanson, integrates the environmental interactions of trace metals with its toxicological effects. This index effectively portrays the potential impact of trace metals on the ecological environment (Yang et al., 2016; Hakanson, 1980). The calculation formulas are as follows:

$$P_i = \frac{C_i}{C_{Bi}} \quad (2)$$

The potential ecological hazard indices for individual trace metals is as follows:

$$E_i = T_i \times P_i \quad (3)$$

The combined potential ecological hazard indices for multiple trace metals is shown below:

$$R_i = \sum_1^n E_i \quad (4)$$

where P_i is the single-factor pollution index of trace metals; C_{Bi} is the background value of trace metal i (mg·kg⁻¹); T_i is the toxicity coefficient of the given trace metal i . The toxicity coefficients are as follows: Cd (30), Hg (40), As (10), Pb (5), Cr (2), Cu (5), Ni (5), and Zn (1) (Hakanson, 1980). The evaluation process is depicted in Fig. S2.

Human health risk assessment

In human health risk assessments, the potential for adverse effects on the population is directly linked to environmental pollutant levels. Following the model outlined by the US Environmental Protection Agency

(USEPA, 1996), which evaluates the health risks associated with soil trace metal exposure in adults and children through three pathways, i.e., oral ingestion, oral nasal inhalation, and dermal contact, the health risks for both adult and child populations were assessed.

Daily exposure to trace metals (mg/kg/day) through three routes, oral ingestion, oral nasal inhalation, and dermal contact, was determined using daily average exposure values (Hossain et al., 2015; USEPA, 1996). SF_i represents the slope factor for metal i , RfD_i represents the reference dose for metal i , and CS represents the trace metals concentration in the soil ($mg \cdot kg^{-1}$). The relevant equations for calculating the daily exposure through oral ingestion, oral-nasal inhalation, and dermal exposure are as follows:

$$ADD_{ing} = \frac{C_s \times IngR \times EF \times ED}{BW \times AT} \times 10^{-6} \tag{5}$$

$$ADD_{inh} = \frac{C_s \times InhR \times EF \times ED}{PEF \times BW \times AT} \tag{6}$$

$$ADD_{dermal} = \frac{C_s \times SA \times AF \times ABS \times EF \times ED}{BW \times AT} \times 10^{-6} \tag{7}$$

$$HI = \sum HQ_i = \sum \frac{ADD_i}{RfD_i} \tag{8}$$

$$THI = \sum HI \tag{9}$$

$$CR_i = \sum ADD_i \times SF_i \tag{10}$$

$$TCRI = \sum CRI = \sum (\sum CR_i) \tag{11}$$

where ADD_{ing} , ADD_{inh} , and ADD_{dermal} are the average daily exposure (mg/kg/day) to trace metals by three routes: oral ingestion, oral-nasal inhalation, and dermal contact, respectively (Hossain et al., 2015; USEPA, 1996); C_s is the content of trace metals in soil ($mg \cdot kg^{-1}$); SF_i is the slope factor for trace metal i ; and RfD_i is the reference dose for metal i . Specific calculation parameters and values are shown in Tables 1 and 2. The evaluation process is depicted in Fig. S3.

Cu, Zn, and Hg do not pose a carcinogenic risk to humans; therefore, no carcinogenic risk calculations are performed for Cu, Zn, and Hg in this paper (Xu et al., 2020; Agency, 2001).

Results and discussion

General characteristics of soil trace metals

Table 3 shows the mean concentrations of soil trace metals in the MRGB, ranked from highest to lowest as follows: Cr (70.88) > Zn (56.8) > Ni (28.63) > Pb (19.40) > Cu (17.64) > As (9.31) > Cd (0.19) > Hg (0.03). Notably, Cr, Zn, Ni, As, Cd, and Hg exhibited higher mean concentrations than background levels in the WFC, indicating varying degrees of accumulation in the MRGB. The coefficient of variation (CV) was significant when the mean value was 0. In our analysis, we observed weak variability for CVs at 0.1, and moderate variability for CVs at 0.11, with Cd (1.14) > Hg (0.8) > Ni (0.67) > Cu (0.39) > Cr

Table 1 Calculation parameters and values of trace metal exposure for adults and children (Agency, 2001)

Parameters	Parameter meanings	Unit	Adult (child) parameter values
IngR	Rate of soil uptake	mg/day	100(200)
ED	Average exposure time	year	26(6)
EF	exposure frequency	day/year	350
BW	Average weight	kg	70(15)
ABS	skin absorption factor	/	0.001
AT	Average exposure time	day	carcinogenic 25550; non-carcinogenic 365×ED
InhR	breath intake	m ³ /day	15(7.5)
SA	Exposed skin area	cm ²	5700(2373)
AF	Skin adhesion factor	mg/cm ²	0.07(0.2)
PEF	Particulate emission factor	m ³ /kg	1.36E+09

Table 2 RfD and SF parameters of trace metals under different exposure pathways (Hall et al., 2000)

	Zn	Ni	Cu	Pb	As	Cr	Cd	Hg
RfD _{ing}	3.00E-01	2.00E-02	4.00E-02	3.50E-03	3.00E-04	3.00E-03	1.00E-03	3.00E-04
RfD _{inh}	3.00E-01	2.06E-02	4.02E-02	3.50E-03	3.00E-04	2.86E-05	1.00E-05	8.57E-05
RfD _{der}	6.00E-02	5.40E-03	1.20E-02	5.25E-04	1.23E-04	6.00E-05	1.00E-05	2.00E-05
SF _{ing}	–	–	–	8.50E-03	1.50E+00	5.00E-01	5.10E-01	–
SF _{inh}	–	8.40E-01	–	–	1.51E+01	4.20E+01	6.30E+00	–
SF _{der}	–	–	–	–	3.66E+00	2.00E+01	2.00E+01	–

“–” no data available

Table 3 General characteristics of soil trace metals in the MRGB

Parameters	Cu	Pb	Zn	Ni	Cr	As	Cd	Hg
Maximum(mg·kg ⁻¹)	46.9	38.16	182.53	138.5	192.3	25.15	2.08	0.18
Minimum(mg·kg ⁻¹)	8.18	8.20	31.92	13.35	46.10	4.01	0.03	0.007
Mean(mg·kg ⁻¹)	17.64	19.40	56.80	28.63	70.88	9.31	0.19	0.03
Standard deviation	6.85	4.41	18.60	19.32	25.65	2.45	0.21	0.03
Coefficient variation	0.39	0.23	0.33	0.67	0.36	0.26	1.14	0.80
Skewness	2.36	1.44	4.03	4.08	3.36	2.89	7.57	3.55
Kurtosis	3.41	1.73	19.72	14.33	8.83	14.59	62.67	14.05
Enrichment factor	0.89	0.96	1.08	1.03	1.09	1.15	2.30	2.11

(0.36) > Zn (0.33) > As (0.26) > Pb (0.23). Notably, Cd exhibited substantial variability, indicating a considerable anthropogenic interference. The degree of trace metal contamination across the MRGB displayed significant spatial heterogeneity, particularly influenced by external factors and potentially altered by human activities, whereas other factors exhibited medium variability. Moreover, the skewness and kurtosis of soil Cd in the MRGB exceeded the typical distribution characteristics of soil trace metals, signifying a more pronounced skewed distribution with elevated concentration extremes. In addition, the kurtosis values of Zn, Ni, As, and Hg are also large, which indicates a flat data distribution, which is quite different from the normal distribution. This deviation may be attributed to the accumulation of trace metals resulting from human activities, which disrupts the normality of the natural distribution.

According to the “Risk Control Standards for Soil Pollution on Agricultural Land of Soil Environmental Quality (Trial)” (GB 15618-2018), the soil in the MRGB exceeds the risk screening values for Ni, Cd, and As by two points each and one point, respectively.

The soil pH significantly affects its physical and chemical characteristics and influences the behavior of trace metals ions, including their enrichment, mobility, and fugacity. The trace metal content in soil varies with pH, with most trace metals indicating a negative

correlation with pH, although certain metals such as Cu and Zn exhibit a positive correlation with pH. In the MRGB, soil pH ranged from 6.79 to 8.69, with an average of 7.85, indicating a weakly alkaline soil. As depicted in Fig. S4, alkaline soils dominated the central region, constituting 97% of the MRGB, whereas acidic soils were concentrated in the northern and southern areas.

Spatial analysis and patterns of soil trace metals content

Geoaccumulation index method

The MRGB generally maintains a non-polluting status, according to the geoaccumulation index approach. However, moderate contamination was observed for Hg (15.31%), Cd (5.10%), Ni (4.08%), Zn (1.02%), and As (1.02%). Hg (2.04%) and Cd (1.02%) exhibited moderate to strong contamination and strong contamination, respectively, indicating that Hg and Cd are the primary pollutants requiring attention and remediation measures. Fig. 2 illustrates the contamination levels assessed using the geoaccumulation index. Notably, Hg exhibited significant anisotropy in its maximum and minimum values, with Cd and Hg showing notably higher anomalies than the other six trace metals.

We generated a cumulative distribution map for Cd and Hg in the MRGB through interpolation based on

inverse distance weights calculated from 98 sampling points. As illustrated in Fig. 3 d and e, Cd pollution was predominantly concentrated in Qianjiazhuang and the vicinity of the Xinfeng Iron and Steel Plant. In contrast, Hg pollution covered a wider area, with notable contamination in Qianjiazhuang and Shouyang Chemical Plant, which served as the most severely affected regions.

The enrichment coefficients for the mean contents of the remaining six trace metals relative to the background values of Weifang soil ranged from 0.89 to 1.15. Notably, with the exception of Cd and Hg, the levels of Cu, Ni, and Cr in the MRGB closely mirrored WFC’s background values of WFC, suggesting primarily natural origins according to the guidelines outlined by Dai et al. (2011) for interpreting enrichment coefficients and source attribution. Conversely, Pb, Zn, and As exhibited enrichment coefficients ranging from 0.96 to 1.15, signifying relative enrichment, implying a potential interplay between natural and anthropogenic sources or purely natural origins. Cd and Hg, on the other hand, demonstrated pronounced enrichment coefficients of 2.30 and 2.11, respectively, indicating conspicuous enrichment and a stronger likelihood of anthropogenic sources.

PERI methodology

The PERI values for trace metals in the MRGB were computed using the formula and Excel. A hierarchical evaluation following the grading criteria in Fig. S2 was conducted for the trace metal PERI values. The ecological risk values for trace metals in the

soil samples are presented in Fig. 2 b and ranked as follows: Hg ($E_i=84.47$) > Cd ($E_i=68.90$) > As ($E_i=11.49$) > Ni ($E_i=5.17$) > Pb ($E_i=4.78$) > Cu ($E_i=4.39$) > Cr ($E_i=2.18$) > Zn ($E_i=1.08$). Within the MRGB, Cu, Ni, Cr, As, Pb, and Zn posed low ecological risks. However, Hg and Cd exhibited varying levels of risk, with 8.38% of Hg samples at moderate risk, 38% at very strong risk, 70% of Cd and Hg samples at moderate risk, 9% at strong risk, 2% at very strong risk, and 1% at extreme risk. In the case of Hg, 38% of the samples exhibited a medium ecological risk, whereas 33% displayed a strong risk, with 5% categorized as very strong and 2% as extremely strong. This distribution was predominantly influenced by the toxicity coefficients of the pollutants, with Cd and Hg demonstrating higher contamination levels and larger toxicity coefficients, resulting in an elevated potential ecological risk. Across all sample sites in the MRGB, the ecological RI ranged from 62.20 to 962.64, with an average value of 182.44, indicating a moderate ecological risk overall. Specifically, 44.9%, 51.02%, and 2.04% of the samples were classified as having low, moderate, and high ecological risks, respectively. Moreover, applying the load pollution index method revealed that all MRGB samples fell within the category of moderate pollution, aligning with assessments of potential ecological risks (Izah et al., 2017; Zhang et al., 2019).

Cd and Hg were the primary contributors to the potential ecological risk of trace metals in the entire MRGB. Therefore, we conducted interpolation and analysis of Cd and Hg to create pollution distribution maps, as shown in Fig. 3 a and b. Cd pollution was

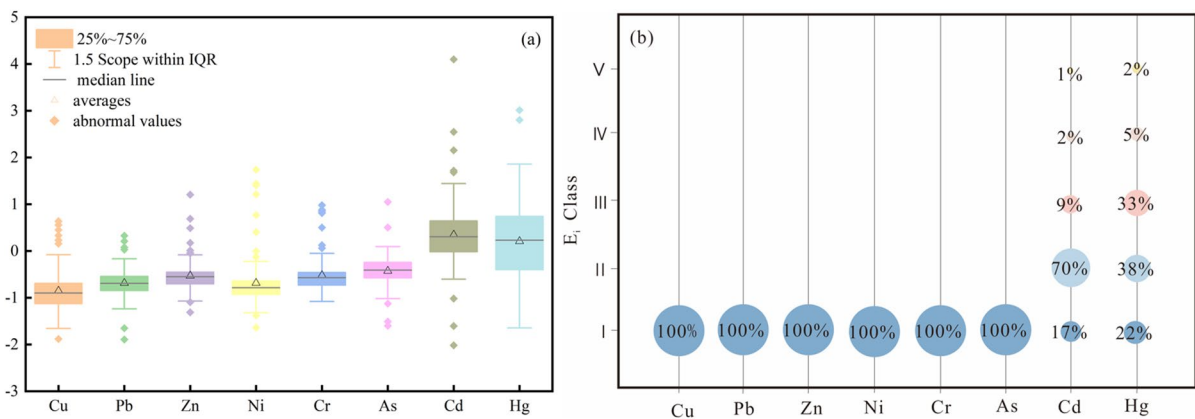


Fig. 2 Box plot of geoaccumulation index method (a) and PERI class distribution (b)

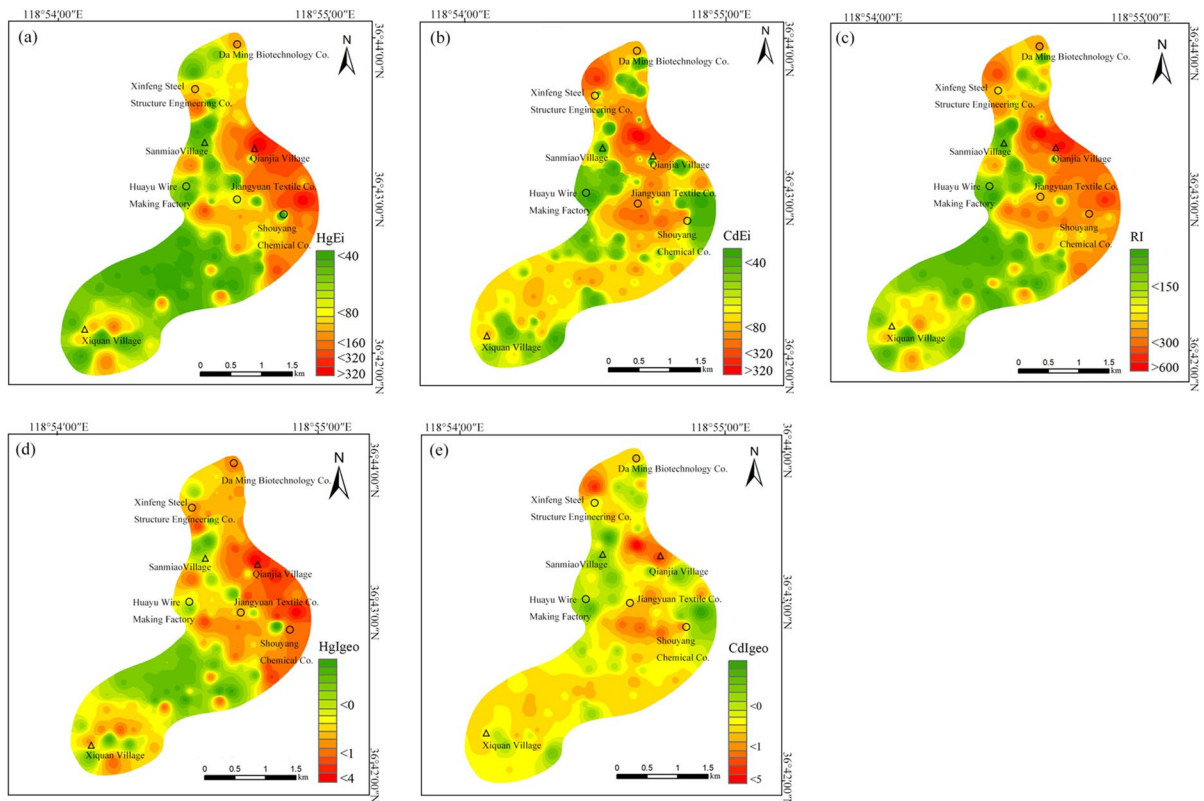


Fig. 3 Distribution of Cd and Hg in relation to PERI and geoaccumulation index

predominantly concentrated around the Xinfeng Iron and Steel Factory, Qianjiazhuang, and Jianguyan Textile Factory, while Hg pollution was most pronounced in the eastern area near Qianjiazhuang and Shouyang Chemical Factory, exhibiting more severe contamination. Fig. 3 c shows these areas, including Daming Biotechnology Co. Ltd., Xinfeng Iron and Steel Plant, Qianjiazhuang, Jianguyan Textile Plant, and Shouyang Chemical Plant, exhibit high values for the comprehensive ecological hazard index. In addition, the southern region of the MRGB shows a relatively lower ecological risk than the more heavily impacted eastern portion.

Evaluation of the potential ecological hazards of soil trace metals throughout the entire research region with regard to human health

Non-carcinogenic risks

In the non-carcinogenic risk assessment of eight trace metals (Cu, Pb, Zn, Ni, Cr, As, Cd, and Hg), the

non-carcinogenic risk values were found to be $THI < 1$ for both adults and children. Specifically, the overall THI non-carcinogenic risk values for adults and children were 9.33×10^{-2} and 8.41×10^{-1} , respectively. These results indicate that the non-carcinogenic risk levels for both adults and children in the MRGB remained within acceptable limits, as outlined in Table 4.

Among all three exposure routes, oral intake was identified as the predominant route of non-carcinogenic risk for both adults and children, ranking higher than dermal contact and oral nasal inhalation. This assessment was based on the non-carcinogenic HQ , where each metal exhibited an HQ value of 1 for both adults and children across all three exposure routes. Oral consumption accounted for a substantial portion of the non-cancer risk quotient (HI), contributing to 99.21% and 98.68% in children and adults, respectively. Notably, children exhibited a higher HI for trace metals Cr and As (>0.1), warranting consideration due to their elevated HQ compared to

Table 4 Evaluation of non-carcinogenic and carcinogenic health risks associated with soil trace metals

	Trace metals	Cu	Pb	Zn	Ni	Cr	As	Cd	Hg
HQ _{ing}	Adult	6.04E-04	7.59E-03	2.59E-04	1.96E-03	3.24E-02	4.25E-02	2.55E-04	3.59E-05
	Children	5.64E-03	7.09E-02	2.42E-03	1.83E-02	3.02E-01	3.97E-01	2.38E-03	3.35E-04
HQ _{inh}	Adult	6.63E-08	8.37E-07	2.86E-08	2.10E-07	3.74E-04	4.69E-06	2.55E-04	1.38E-08
	Children	1.55E-07	1.95E-06	6.67E-08	4.90E-07	8.74E-04	1.09E-05	2.38E-03	3.23E-08
HQ _{der}	Adult	8.03E-06	2.02E-04	5.17E-06	2.89E-05	6.46E-03	4.14E-04	2.81E-06	2.15E-06
	Children	4.46E-05	1.12E-03	2.87E-05	1.61E-04	3.58E-02	2.30E-03	6.56E-06	1.19E-05
HI	Adult	6.12E-04	7.79E-03	2.65E-04	1.99E-03	3.92E-02	4.29E-02	5.12E-04	3.80E-05
	Children	5.68E-03	7.20E-02	2.45E-03	1.85E-02	3.39E-01	3.99E-01	4.76E-03	3.47E-04
CR _{ing}	Adult	–	8.39E-08	–	–	1.8E-05	7.1E-06	4.83E-08	–
	Children	–	1.81E-07	–	–	3.88E-05	1.53E-05	1.04E-07	–
CR _{inh}	Adult	–	–	–	1.35E-09	1.67E-07	7.89E-09	6.58E-11	–
	Children	–	–	–	7.27E-10	9E-08	4.25E-09	3.54E-11	–
CR _{der}	Adult	–	–	–	–	2.88E-06	6.92E-08	7.55E-09	–
	Children	–	–	–	–	3.69E-06	8.86E-08	9.68E-09	–
CRI	Adult	–	8.39E-08	–	1.35E-09	2.11E-05	7.18E-06	5.59E-08	–
	Children	–	1.81E-07	–	7.27E-10	4.26E-05	1.54E-05	1.14E-07	–

adults. The relative contributions of the HI values of each trace metals to the overall non-carcinogenic risk index THI in adults and children are presented in Fig. S5. It is evident that Cr and As have a significantly greater impact than other trace metals. Overall, this study indicates that neither adults nor children in the MRGB face significant noncarcinogenic risks. However, it also highlights Cr and As as the most influential non-carcinogenic risk factors for both adults and children, necessitating preventive measures.

Risk of carcinogens

Table 4 reveals that the TCRI values for the five carcinogenic trace metals in the MRGB, considering three exposure pathways, were 2.84E-05 for adults and 5.83E-05 for children. These values fall within the acceptable range for carcinogenic risk to human health (1×10^{-6} – 1×10^{-4}) to human health. This study focused on evaluating the carcinogenic risks of five trace metals: Ni, Pb, As, Cr, and Cd. Notably, the TCRI values were higher for children than for adults, signifying that the carcinogenic risk associated with soil trace metals in the MRGB was within acceptable limits for both local adults and children.

For each exposure route, the CR values of the five trace metals fell within the range of no carcinogenicity risk ($< 1 \times 10^{-6}$) and tolerable carcinogenicity

risk for humans. Comparative analysis revealed that children had lower CR values than adults for each trace metals in both oral and dermal exposure routes, as well as lower CR values for oral-nasal exposure. Additionally, for As, Cr, and Cd, the risk hierarchy was oral consumption > skin contact > oral/nasal inhalation, highlighting oral intake as the predominant route of carcinogenic health risk.

The oral route significantly contributed to carcinogenicity risk, accounting for 85.55% of adults and 91.14% of children, which was notably higher in children. In each exposure pathway, the CR values for the five trace metals fell within the range of no carcinogenic risk ($< 1 \times 10^{-6}$) and a tolerable level for human health. The analysis indicated that children exhibited lower CR values than adults for both oral and dermal exposure routes, as well as lower CR values for oral-nasal exposure. Specifically, for As, Cr, and Cd, the risk hierarchy was oral consumption > skin contact > oral/nasal inhalation, underscoring oral intake as the primary route of carcinogenic health risks.

Table 4 presents the CRIs for the adults and children. Notably, the CRIs for all trace metals, except Ni, were lower in adults, as only the CRI for Ni was calculated for the oral and nasal inhalation routes. The CRI values for both adults and children followed the order Cr > As > Pb > Cd > Ni. Specifically, CRI

values for As and Cr in adults and children were within acceptable cancer risk levels, whereas Cd, Pb, and Ni CRI values posed no health risks. Fig. S6 illustrates that Cr made a substantial contribution to the overall cancer risk, accounting for 74.33% and 73.09% in adults and children, respectively. Based on these findings, Cr, a trace metals present in the soil, has emerged as the primary contributor to cancer risk in MRGB. It is evident that neither adults nor children in the MRGB face significant carcinogenic risk.

A comparison of trace metals levels between the MRGB and Pakistani regions reveals that the MRGB experienced lower contamination levels. It primarily exhibited mild contamination in terms of geoaccumulation index and potential ecological risk, resulting in a lower risk to human health. In contrast, the Pakistani region demonstrated higher geoaccumulation index values, ecological risks, and greater threats to human health. However, oral intake remained the primary route of health risks in both regions, with children being more vulnerable to trace metal exposure. Notably, As emerged as a significant non-carcinogenic risk factor in both areas.

Tracing the sources of trace metals in soil

Analysis of correlation

The correlation analysis of soil trace metals in the MRGB, conducted using Spearman's correlation test, is detailed in Table 5. The analysis indicated significant relationships between various trace metals. Notably, strong correlations existed among Cu, Zn, Ni, Cr, As, and Cd, as well as between Hg and Pb, As, and Zn. These findings are visually represented in Fig. 4, which depicts the regional distribution of pollution for each trace metal component.

Table 5 Correlations among trace metals in soil

	Cu	Pb	Zn	Ni	Cr	As	Cd	Hg
Cu	1							
Pb	0.27	1						
Zn	.519**	.318**	1					
Ni	.591**	0.399	.417**	1				
Cr	.608**	0.121	.419**	.772**	1			
As	.314**	0.831	0.128	.360**	.329**	1		
Cd	.333**	0.204	.429**	0.058	.255**	0.943	1	
Hg	0.971	.439**	.290**	0.332	0.924	-.255*	0.181	1

**Significant correlation at the 0.01 level (two-tailed); *significant correlation at the 0.05 level (two-tailed)

Principal component analysis

Principal component analysis (PCA) effectively integrates influencing factors, identifies the most significant contributing factors, simplifies the data structure, and enhances source identification. Notably, the KMO value was 0.643, exceeding the threshold of 0.5, and Bartlett's sphericity test result of 0.001 confirmed the suitability of PCA for analyzing the dataset.

The results are presented in Table 6. Our analysis extracted three principal components that collectively explained 81.1% of the total data variance. These components form the basis for understanding the sources of trace metals in the soil and their distribution patterns. The first principal component, explaining 36.75% of the variance, featured key loadings for Cu (0.881), Zn (0.626), Ni (0.930), and Cr (0.925), all of which exhibited significant positive correlations at $P \leq 0.01$ level. Notably, the high loadings and correlations of Cu, Ni, and Cr suggested the same source. Additionally, Zn demonstrated substantial loading (0.703) in the second principal component. The second principal component, responsible for 28.41% of the total variance, exhibited significant loadings in Pb (0.816), Zn (0.703), Cd (0.739), and Hg (0.658). The third principal component, which explained 12.94% of the variance, was primarily loaded with As (0.904).

Cluster analysis

Cluster analysis leverages the strong similarity among trace metals within the same category and their minimal similarity across different categories to classify the data. The results of the cluster analysis for the eight trace metals in the soil, utilizing the intergroup linkage method, are depicted in Fig. 5. The data were

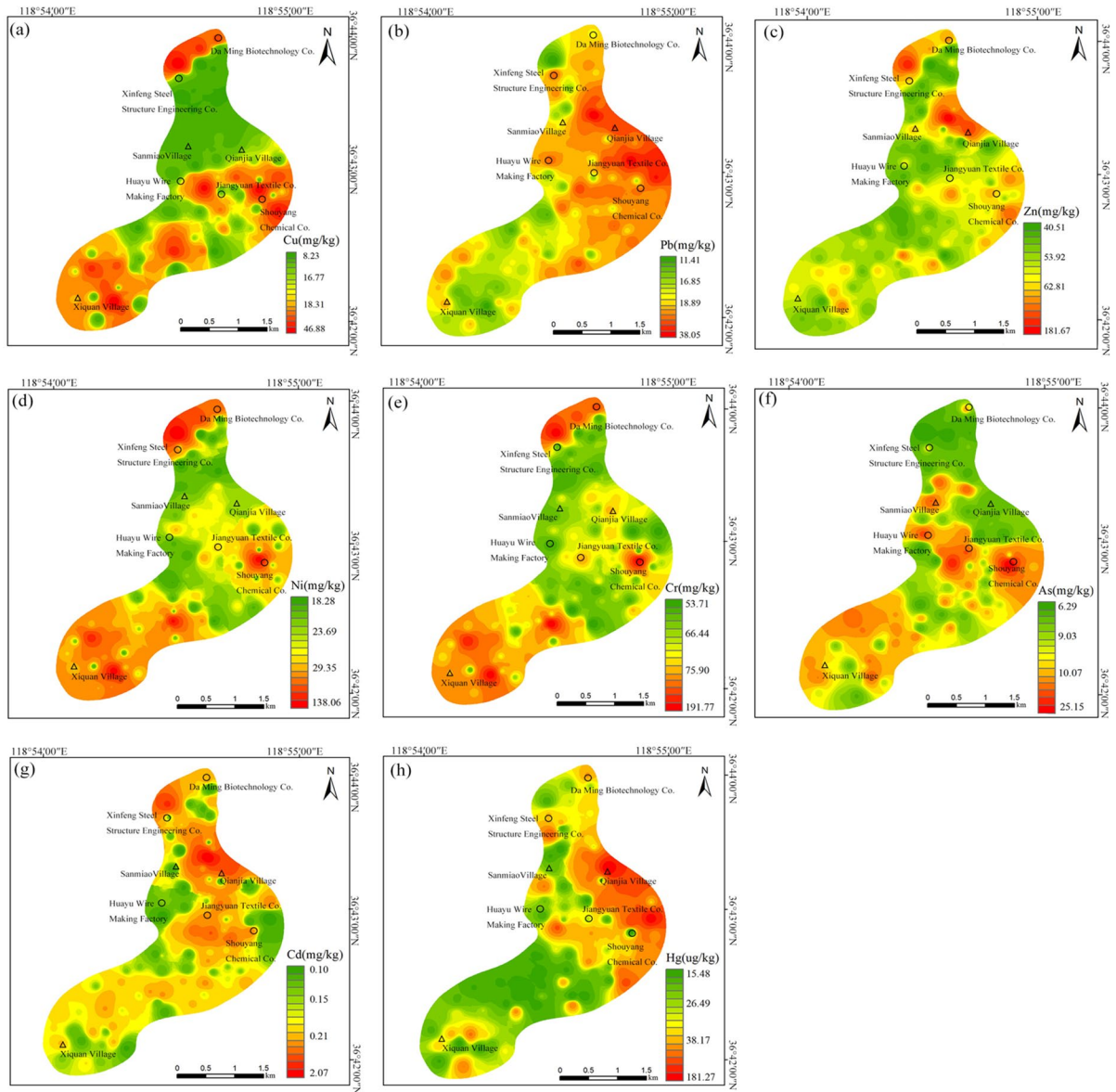


Fig. 4 Spatial distribution of soil trace metals

categorized into three groups, each corresponding to one of three principal components: PC1, PC3, and PC2. The separation between these groups was maintained within the range of 15–20 units.

Source identification

Soil trace metal sources can be categorized as anthropogenic or natural, and their identification relies on geostatistical analysis and spatial distribution

patterns of trace metals. The PC1 factor loadings were predominantly associated with Cu, Zn, Ni, and Cr. Examining the spatial arrangement in Fig. 4, the regions with high values for these three trace metals, Cu, Ni, and Cr, were roughly distributed in specific areas. These areas included the east-west belt near Daming Biotechnology Co. Ltd., the central region near the Jiangyuan Textile Factory and Shouyang Chemical Factory, and the southern region between Yite Technology Co. and Xiquan Village.

Table 6 PCA of surface soil trace metals

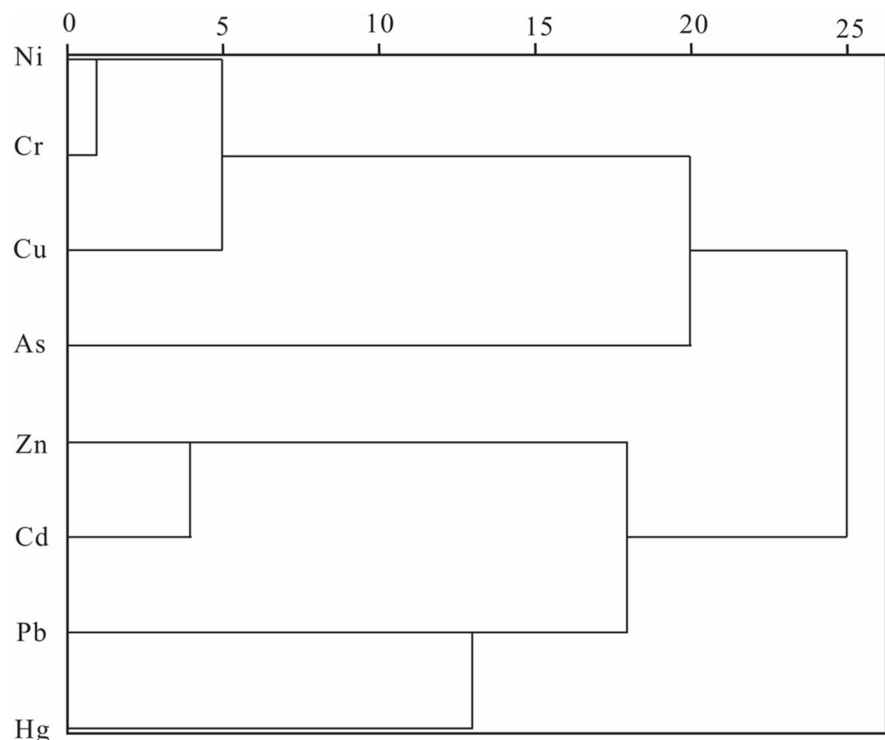
Metals	PCA		
	PC1, Cu, Zn, Ni, Cr	PC2, Pb, Zn, Cd, Hg	PC3, As
Cu	0.881	-0.153	0.021
Pb	-0.150	0.816	0.263
Zn	0.626	0.703	-0.110
Ni	0.930	-0.230	-0.147
Cr	0.925	-0.238	-0.114
As	0.328	-0.028	0.904
Cd	0.399	0.739	0.049
Hg	-0.050	0.658	-0.314
Variances %	39.75	28.41	12.94
Cumulative variance %	39.75	68.16	81.10
Eigenvalue	3.18	2.27	1.04

Additionally, variations in the contents of these four trace metals across different regions suggested that they primarily originated from soil parent materials. Other studies have demonstrated the influence of soil parent materials and rocks on trace metal distribution (Bhupander et al., 2012., Gasiorek et al., 2017).

The factor loadings of PC1 were mainly associated with trace metals Pb, Zn, Cd, and Hg concentrations.

The spatial distribution of these four trace metals exhibited a relatively consistent pattern, with most of the concentration centers overlapping. These concentrations were predominantly located in the northern region near Daming Biotechnology Co. and Xinfeng Iron and Steel Factory, as well as in the central-eastern part of Qianjiazhuang, Jiangyuan Textile, and Shouyang. This suggests that the primary contributing factors were industrial pollution, transportation, and the application of agricultural manure and fertilizers. Therefore, in addition to natural sources of Zn, anthropogenic influences, such as industrial emissions and transportation, play a significant role in the distribution of these trace metals.

The spatial distribution of arsenic is concentrated primarily in the vicinity of the Huayi Electric Wire Factory, Jiangyuan Textile Factory, and Shouyang Chemical Factory in the central region, as well as in the southern part near Yite Technology and West Circle Village. Unlike Cu, Ni, and Cr, which are identified as anthropogenic source factors with a clear distribution in the northern region, As' distribution is not well-defined in the north. This suggests that the primary contributing factors are industrial pollution, transportation, and the application of manure and

Fig. 5 R-type clustering of trace metals in surface soils

fertilizers in agriculture (Yang et al., 2022). Transportation, industrial emissions, and coal combustion were the main anthropogenic sources of As. Given the prevalence of mining, industrial activities, and transportation operations in the area, coupled with the fact that communities and industries constitute the majority of the anomalous area for As, these three factors are considered the primary anthropogenic sources of As in the MRGB.

Conclusions

Given the significance of agricultural activities in the MRGB, soil quality is of paramount importance. This study comprehensively assessed soil trace metal pollution, including its characteristics, underlying causes, and associated health risks, in the MRGB. The key findings are summarized as follows:

- (1) Except for a few isolated points with Ni, Cr, and As, the average soil trace metal levels in WFC exceeded the background values, whereas Cu and Pb contents were lower. For all other trace metals at every point, the levels were below the national risk screening values, signifying localized high trace metal concentrations in certain areas of the MRGB.
- (2) The geoaccumulation index indicated that Cd and Hg were the most frequently occurring pollutants. More than 90% of the points exhibited non-pollution levels for Cu, Pb, Zn, Ni, Cr, and As. In terms of potential ecological risk, Hg had the highest single potential ecological risk index (84.47), reaching a strong ecological hazard level, followed by Cd (68.90) at a moderate ecological hazard level. The other six trace metals had low ecological hazard levels. Overall, the composite ecological hazard index for the MRGB fell into the medium ecological risk category.
- (3) The non-carcinogenic risk assessment indicated that soil trace metals in the MRGB posed acceptable health risks to both adults and children. As and Cr were the main non-carcinogenic risk factors that significantly contributed to the risk in both groups. In terms of carcinogenic risk, the overall risk for both adults and children was within tolerable limits, with Cr being the primary contributor. Oral ingestion was the main exposure route for both carcinogenic and non-carcinogenic hazards.
- (4) In the MRGB's soil, Cu, Zn, Ni, and Cr were predominantly sourced from natural parent rocks, except for Zn, which also exhibited influence from industrial emissions and traffic-related anthropogenic sources. Pb, Cd, and Hg were primarily affected by traffic and the application of manure fertilizers and agricultural chemicals. As, on the other hand, was primarily attributed to coal combustion and industrial emissions.

Author contribution Zongjun Gao: supervision, writing—original draft.

Menghan Tan: formal analysis, software, methodology, writing—original draft.

Jiutan Liu: research, conceptualization, methodology, writing review, resource acquisition.

Yuqi Zhang: investigation, resource acquisition.

Yiru Niu: investigation.

Bing Jiang: investigation, resource acquisition.

All the authors have read and agreed to the published version of the manuscript.

Funding This study received support from the Geological Exploration and Scientific and Technological Innovation Project of Shandong Provincial Bureau of Geology and Mineral Resources (202005) and the Research on Major Geological Environmental Issues in the Coastal Zone of Shandong Province (KY201911).

Data availability Data will be made available on request, but are available from the corresponding author on reasonable request.

Declarations

Competing interests The authors declare no competing interests.

Ethics approval All authors have read, understood, and complied with the Instructions for Authors' statement on "Ethical Responsibilities of Authors" as necessary.

References

- Agency. (2001). Supplemental Guidance for Developing Soil Screening Levels for Superfund Sites. *Office of Emergency and Remedial Response US Environment Protection Agency Washington, DC 20460*. OSWER 9355.4-24.
- Bhupander, K., Gargi, G., Richa, G., Dev, P., & Shekhar, S. C. (2012). Distribution, composition profiles and source identification of polycyclic aromatic hydrocarbons in roadside soil of Delhi, India. *Journal of Environment & Earth Science*, 2(1), 10–22.
- Chen, T. B., Zheng, Y. M., Lei, M., Huang, Z. C., & Tian, Q. Z. (2005). Assessment of heavy metal pollution in surface soils of urban parks in Beijing. *China. Chemosphere*,

- 60(4), 542–551. <https://doi.org/10.1016/j.chemosphere.2004.12.072>
- Dai, J. R., Pang, X. G., Yu, C., Wang, C. L., & Hu, X. P. (2011). Geochemical baselines and background values and element enrichment characteristics in soils in Eastern Shandong Province. *Geochimica*, 40(6), 577–581. <https://doi.org/10.1007/s11629-011-2067-x>
- Delavar, M., & Safari, Y. (2016). Spatial distribution of heavy metals in soils and plants in Zinc Town, Northwest Iran. *International Journal of Environmental Science & Technology*, 13(1), 297–306. <https://doi.org/10.1007/s13762-015-0868-0>
- Din, I. U., Muhammad, S., & Rehman, I. U. (2022). Heavy metal(loid)s contaminations in soils of Pakistan: A review for the evaluation of human and ecological risks assessment and spatial distribution. *Environmental Geochemistry and Health*, 45(5), 1991–2012. <https://doi.org/10.1007/s10653-022-01312-x>
- Ferreira-Baptista, L., & Miguel, E. D. (2005). Geochemistry and risk assessment of street dust in Luanda, Angola: A tropical urban environment. *Atmospheric Environment*, 39(25), 4501–4512. <https://doi.org/10.1016/j.atmosenv.2005.03.026>
- Flora, A., Emma, F., Beatriz, C., & María, L. (2009). Enrichment of marsh soils with heavy metals by effect of anthropic pollution. *Journal of Hazardous Materials*, 170(2–3), 1056–1063. <https://doi.org/10.1016/j.jhazmat.2009.05.074>
- Gasiorek, M., Kowalska, J., Mazurek, R., & Pajak, M. (2017). Comprehensive assessment of heavy metal pollution in topsoil of historical urban park on an example of the Planty Park in Krakow (Poland). *Chemosphere*, 179(Jul), 148–158. <https://doi.org/10.1016/j.chemosphere.2017.03.106>
- Govil, P. K., Sorlie, J. E., Murthy, N. N., Sujatha, D., Reddy, G. L. N., Rudolph-Lund, K., Krishna, A. K., & Mohan, K. R. (2008). Soil contamination of heavy metals in the Katedan Industrial Development Area, Hyderabad. *India. Environmental Monitoring and Assessment*, 140(1–3), 313–323. <https://doi.org/10.1007/s10661-007-9869-x>
- Guseva, A. S., & Petrov, V. A. (2023). Assessment of soil pollution by heavy metals in certain areas of New Moscow. *Doklady Earth Sciences*, 510(1), 353–357. <https://doi.org/10.1134/S1028334X23600202>
- Hakanson, L. (1980). An ecological risk index for aquatic pollution control, a sedimentological approach. *Water Research*, 14(8), 975–1001. [https://doi.org/10.1016/0043-1354\(80\)90143-8](https://doi.org/10.1016/0043-1354(80)90143-8)
- Hall, R. K., Wolinsky, G. A., & Husby, P. (2000). Status of aquatic bioassessment in U.S. EPA Region IX. *Environmental Monitoring & Assessment*, 64(1), 17–30. <https://doi.org/10.1023/A:1006430231539>
- Hossain, M. A., Ali, N. M., Islam, M. S., & Hossain, H. M. Z. (2015). Spatial distribution and source apportionment of heavy metals in soils of Gebeng Industrial City. *Malaysia. Environmental Earth Sciences*, 73(1), 115–126. <https://doi.org/10.1007/s12665-014-3398-z>
- Izah, S. C., Basse, S. E., & Ohimain, E. I. (2017). Assessment of pollution load indices of heavy metals in cassava mill effluents contaminated soil: A case study of small-scale processors in a rural community in the Niger Delta. *Nigeria. Bioscience Methods*, 8(1), 542–551. <https://doi.org/10.5376/bm.2017.08.0001>
- Jadoon, S., Muhammad, S., Hilal, Z., Ali, M., Khan, S., & Khatkhat, N. U. (2020). Spatial distribution of potentially toxic elements in urban soils of Abbottabad City, (N Pakistan): Evaluation for potential risk. *Microchemical Journal*, 153, 104489. <https://doi.org/10.1016/j.microc.2019.104489>
- Khan, S. A., Muhammad, S., Nazir, S., & Shah, F. A. (2020). Heavy metals bounded to particulate matter in the residential and industrial sites of Islamabad, Pakistan: Implications for non-cancer and cancer risks. *Environmental Technology & Innovation*, 19, 100822. <https://doi.org/10.1016/j.eti.2020.100822>
- Lee, H. G., Kim, H. K., Noh, H. J., Byun, Y. J., Chung, H. M., & Kim, J. I. (2020). Source identification and assessment of heavy metal contamination in urban soils based on cluster analysis and multiple pollution indices. *Journal of Soils and Sediments*, 21(5), 1947–1961. <https://doi.org/10.1007/s11368-020-02716-x>
- Lin, J., Zhang, Z. C., & Qiu, Q. (2001). Assessment on pollution of heavy metal in soil along road with method of the index of geo-accumulation. *Practical Preventive Medicine*, 8(5), 339–340.
- Mohammed, L., Benhaddya, M., & Hadjel, M. (2014). Spatial distribution and contamination assessment of heavy metals in surface soils of Hassi Messaoud Algeria. *Environmental Earth Sciences*, 71(3), 1473–1486. <https://doi.org/10.1007/s12665-013-2552-3>
- Muhammad, S. (2022). Evaluation of heavy metals in water and sediments, pollution, and risk indices of Naltar Lakes Pakistan. *Environmental Science and Pollution Research*, 30(10), 28217–28226. <https://doi.org/10.1007/s11356-022-24160-9>
- Naveedullah, Hashmi, M. Z., Yu, C., Shen, H., Duan, D., Shen, C., Lou, L., & Chen, Y. (2013). Risk assessment of heavy metals pollution in agricultural soils of Siling reservoir watershed in Zhejiang Province, China. *BioMed Research International*, 2013(0), 590306. <https://doi.org/10.1155/2013/590306>
- Reimann, C., & Caritat, P. (2005). Distinguishing between natural and anthropogenic sources for elements in the environment: Regional geochemical surveys versus enrichment factors. *Science of the Total Environment*, 337(1–3), 91–107. <https://doi.org/10.1016/j.scitotenv.2004.06.011>
- Sun, Y., Zhou, Q., Xie, X., & Liu, R. (2010). Spatial, sources and risk assessment of heavy metal contamination of urban soils in typical regions of Shenyang. *China. Journal of Hazardous Materials*, 174(1–3), 455–462. <https://doi.org/10.1016/j.jhazmat.2009.09.074>
- Taghipour, H., Mosaferi, M., Armanfar, F., & Gaemmagami, S. J. (2013). Heavy metals pollution in the soils of suburban areas in big cities: A case study. *International Journal of Environmental Science & Technology*, 10(2), 243–250. <https://doi.org/10.1007/s13762-012-0143-6>
- Tian, K., Huang, B., Xing, Z., & Hu, W. Y. (2017). Geochemical baseline establishment and ecological risk evaluation of heavy metals in greenhouse soils from Dongtai. *China. Ecological Indicators*, 72(1), 510–520. <https://doi.org/10.1016/j.ecolind.2016.08.037>
- Ullah, R., & Muhammad, S. (2020). Heavy metals contamination in soils and plants along with the Mafic-ultramafic Complex (Ophiolites), Baluchistan, Pakistan: Evaluation for risk and phytoremediation potential. *Environmental Technology & Innovation*, 19, 100931. <https://doi.org/10.1016/j.eti.2020.100931>

- USEPA. (1996). Exposure Factors Handbook. *U.S. Environmental Protection Agency, Washington, DC*. EPA/600/P-95/002F a-c.
- Xu, X., Han, J., Pang, J., Wang, X., & Qiu, G. (2020). Methylmercury and inorganic mercury in Chinese commercial rice: Implications for overestimated human exposure and health risk. *Environmental Pollution*, 258, 113706. <https://doi.org/10.1016/j.envpol.2019.113706>
- Yang, Z., Di, W. U., Xiang, Z., Kang, C., Wang, F., Huang, Z., & Zhang, L. (2016). Evaluation on potential ecological risk of heavy metals in soil from Penglai Fairyland Park. *Asian Agricultural Research*, 8(6), 75–86.
- Yang, H., Dong, C., Zhang, H., Luo, H., Li, J., Yin, J., Dong, X., Wei, Z., Zhang, N., & Bao, L. (2022). Characteristics and source analysis of soil heavy metal pollution in a mining area. *Journal of Geoscience and Environment Protection*, 10(3), 159–176. <https://doi.org/10.4236/gep.2022.103012>
- Zhang, H., Li, Q., Ji, H., & Lu, K. (2019). Evaluation of heavy metal pollution in farmland soil of Henan Province based on bibliometrics. *Hans Journal of Agricultural Sciences*, 9(1), 55–64. <https://doi.org/10.12677/HJAS.2019.91010>

Publisher's Note Springer Nature remains neutral with regard to jurisdictional claims in published maps and institutional affiliations.

Springer Nature or its licensor (e.g. a society or other partner) holds exclusive rights to this article under a publishing agreement with the author(s) or other rightsholder(s); author self-archiving of the accepted manuscript version of this article is solely governed by the terms of such publishing agreement and applicable law.